SUPPLEMENTAL MATERIAL

Specimen preparation for ex vivo imaging

The imaging data was obtained in a previous study using high-resolution late gadolinium and diffusion tensor MRI[1]. In summary, in n=8 Yorkshire porcines, the mid-left anterior descending coronary artery (LAD) was occluded for 120 mins to create anterioapical infarction. The porcine gross anatomy and its coronary microvasculature have been shown to be very similar to those of humans[2,3]. As a gold standard for myocardial infarction imaging, Gd-DTPA (Magnevist®) was injected (0.2 mmol/kg) through Intravenous (IV) line 20 minutes before animal sacrifice. Under anesthesia, the animals were injected with heparin to prevent clot formation in the heart. After excision, the ventricles were filled with rubber (Task5^{TM}) to keep the heart in the natural unloaded shape. To avoid sample dehydration and susceptibility artifacts generated from the tissue-air interface, the hearts were submerged in perfluorocarbon, (Fluorinert-77, 3M) prior to subsequent imaging sessions.

VT induction in the models

The scar tissue was modeled as an electrical insulator by removing the scar internal nodes from the ventricular mesh. For the purpose of inducing monomorphic sustained VTs only, so that the geometrical contributions of the scar distribution to arrhythmia can be studied, the nodes within a single border layer around the 3D scar were assigned a lower conduction velocity and a longer action potential duration[4]. The latter assumption ensured that unidirectional block took place following the pacing protocol described in the Methods (see Figure S1). VTs continue to perpetuate through the same pathways upon removal of this assumption.

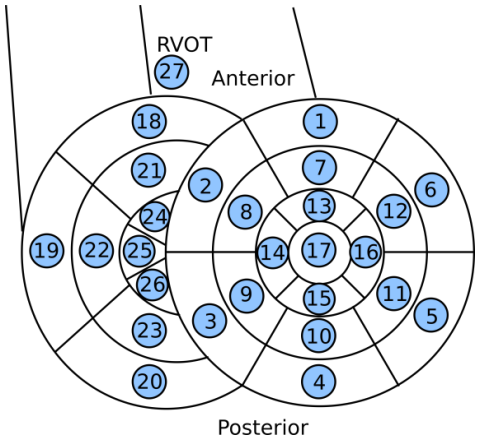

Figure S1. Schematic for assignment of pacing locations based on a modified AHA segment annotation.

Calculation of viable tissue thickness

To characterize the structure of the surviving tissue surrounding the scar, we defined a new *scar-mapped local thickness* (SMLT) metric. This metric was calculated for each node on the 3D scar surface as described below.

First a Euclidean distance map was created by assigning to all the myocardium nodes in the ventricular mesh a value equal to the shortest distance to a boundary surface; here a boundary surface was either the interface of scar and myocardium (scar surface), or the epicardial and endocardial surfaces. Second, at each node on the 3D scar surface, a line was extended within the myocardium in the direction normal to the surface (Figure S2) until it intersected with another boundary surface. The thickness metric was defined to be the minimum of the two values, l and $2d_{max}$, where l is the length of the normal line described above and d_{max} is the maximum of the distance map values calculated at the tissue points traversed by the normal line. In the cases where the local normal to a given surface ends up being nearly perpendicular to the surfaces it intersects, l is an accurate representation of the surviving tissue thickness (Figure S2: l in bottom right). However, in cases where the normal line is oblique to the boundary surface it intersects, it will overestimate the thickness (Figure S2: l' in the bottom left); in this case $2d_{max}$ is selected as the thickness value (as an approximation of the diameter of the largest circle inscribed within the surviving tissue that is tangential to the scar surface node). This method thus provides a metric to quantify the thickness of the surviving tissue surrounding the scar. SMLT values above 10 mm were not included in calculating the aggregated statistics (comprised only 2% of the data).

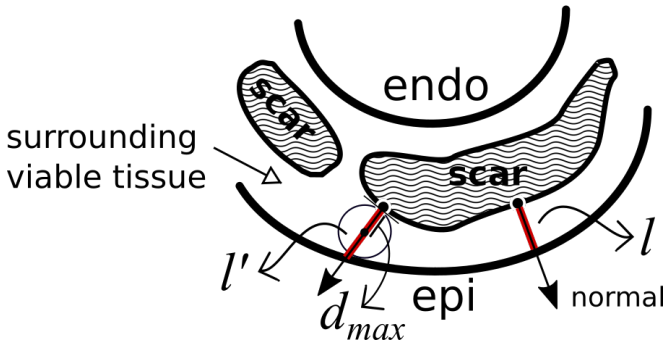

Figure S2. Schematic for SMLT calculation. The process has been illustrated for two representative nodes on the scar (the black arrow lines represent the normal vector to the surface, and the red segments denote the length of the normal between the two boundary surfaces). l and l' are the lengths of the red segments for two cases (see text for detail). The circle on the left shows the largest circle inscribed within the surviving tissue tangential to the scar surface node. d_{max} is the radius of the circle.

Paced propagation in ventricular models

Figure S3 presents paced propagation in two infarcted heart models. Geometries of the 3D heart models are presented in Figure S3-A, showing also the scar color-coded by SMLT values. The activation isochronal maps (Figure S3-B) demonstrate regional activation heterogeneity in the zone of infarct. This heterogeneity is imposed by the complex distribution of the scar and surviving tissue, with isochrone bunching in thin surviving tissue. As demonstrated in heart 5, a thicker region of surviving tissue at the septum (with thickness values of >1 mm) sustains faster propagation relative to those of remote tissue, exacerbating heterogeneity.

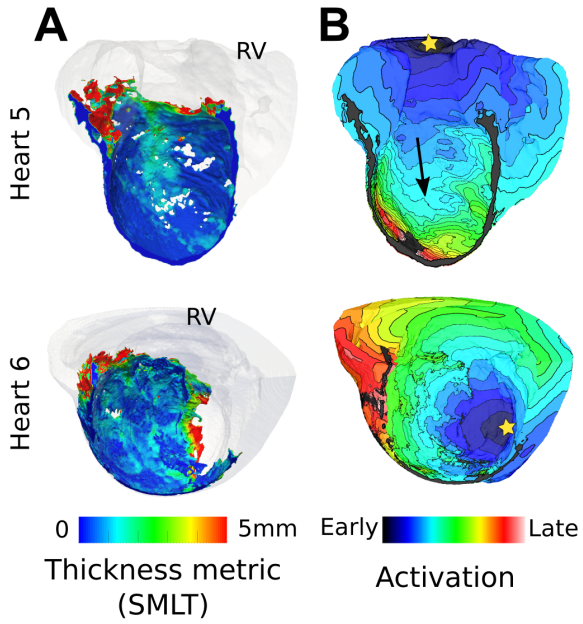

Figure S3. Paced propagation in two infarcted heart models. Results are rendered on a cross-section through the ventricles, with the LV endocardium (septum) exposed. **(A)** 3D ventricular geometry with the scar color-coded with the SMLT metric. Viable tissue is rendered in transparent gray. **(B)** Activation isochrones maps. Stars denote pacing locations. Consecutive contours are 13.3 ms apart.

VT characteristics

Table S1 provides the VT characteristics for the 23 individual VT morphologies in our study. All the VTs in the table were monomorphic and sustained for at least 2 s after the last pacing stimulus. The VTs had an average cycle length (CL) of 190 ± 59 ms, and a mean path length of 53 ± 14 mm. The average conduction velocity on the pathways was 30 ± 8 cm/s. The CL demonstrated a weak to moderate positive correlation with the path length (Pearson correlation = 0.41).

VT #	Heart no.	Pacing Sites	Transmural location (Endo/Trans/Epi)	CL (ms)	Path Length (mm)
1	1	22,24	Epicardial	135	43.7
2	2	11	Endocardial	135	62.5
3	3	10,22,25	Epicardial	135	47.6
4	4	1,6	Endocardial	180	58.7
5	4	2-5,7,10, 11,20,21,27	Endocardial	190	43.4
6	4	8,9,14,15, 17-19,22-26	Transmural/Epi/Endo	210	68.6
7	4	12	Endocardial	245	43.2
8	4	13	Endocardial	355	49.8
9	4	16	Endocardial	205	35.5
10	5	4	Epicardial	230	73.9
11	5	8	Transmural/Epi/Endo	145	51.5
12	5	12	Endocardial	260	64.9
13	5	21,24	Transmural/Epi/Endo	140	58.4
14	6	5,18,19	Endocardial	295	95.2
15	6	8,13,21,23	Endocardial	165	55.3
16	6	15	Endocardial	145	43.4
17	7	1,5-7,10-13,15-17	Transmural/Epi/Endo	240	58.4
18	7	2-4,8,9,26	Transmural	155	46.7
19	7	25	Transmural/Epi/Endo	160	36.6
20	8	5,6,11,13,16	Epicardial	200	52.6
21	8	7	Endocardial	175	38.2
22	8	20	Epicardial	130	48.5
23	8	23	Endocardial	140	48.6
			MEAN ± SD	190 ± 59	53 ± 14

Table S1 Summary of all induced VTs in all models. Pacing sites column presents the locations (see Figure S2 for the definition of site numbers) from which a particular VT morphology was induced. Transmural location column classifies VTs on the basis of wall location relative to the scar (e.g. Endocardial means reentry perpetuated on the endocardial side of the scar). CL: Cycle length.

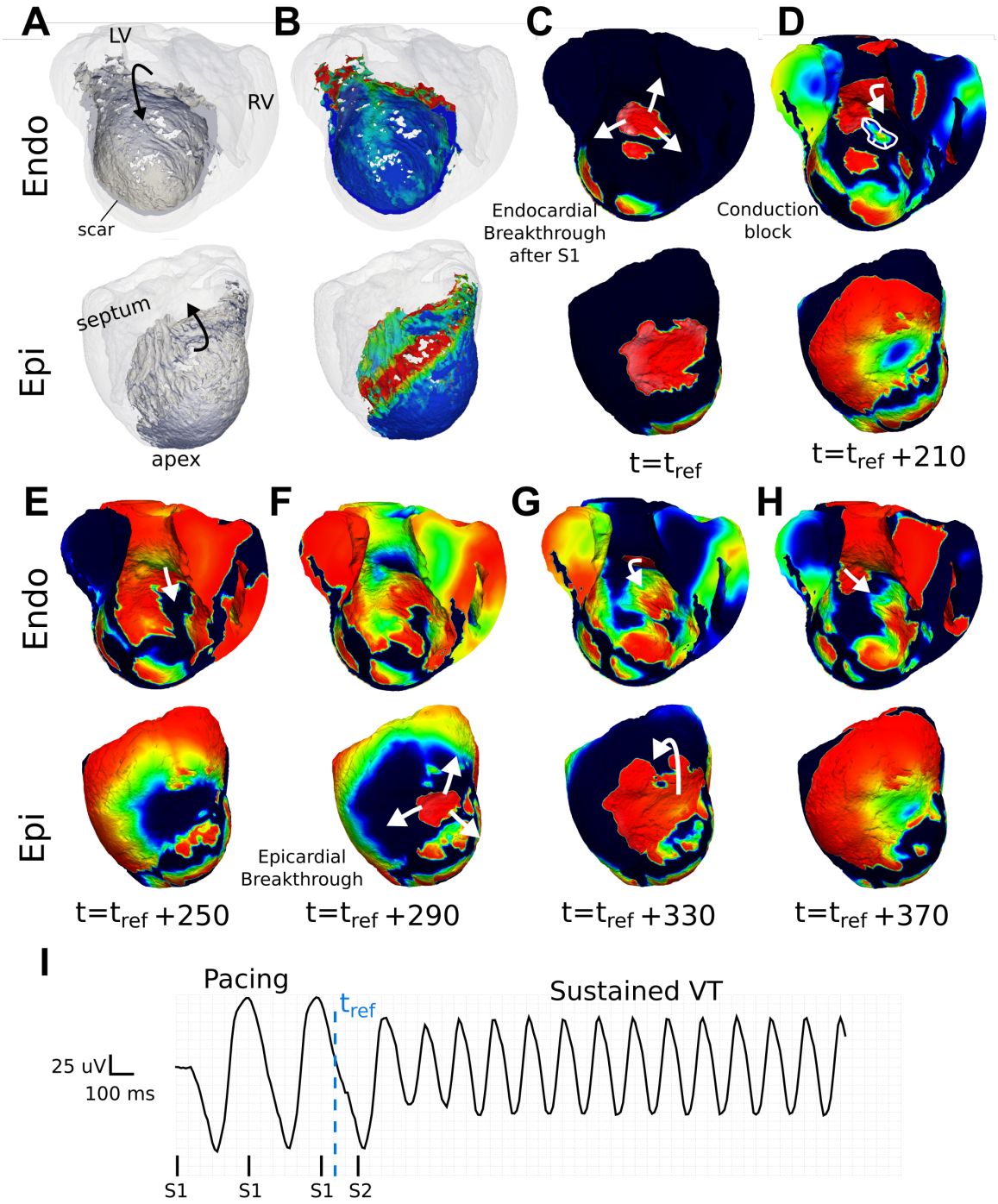

Figure S4 An example of VT (VT #11) with breakthroughs on the epicardial and endocardial surfaces in heart 5 (CL = 145 ms). **(A)** 3D heart geometry **(B)** 3D geometry but with the scar color-coded with the thickness metric **(C)** Endocardial breakthrough following S1 pacing. The breakthrough happens after the wave exits a transmural viable tissue within the infarct. **(D)** Conduction block at the endocardial side of the transmural surviving tissue. **(E-H)** Sustained reentry traversing both the sub-endocardial and the sub-epicardial tissues **(I)** Pseudo-ECG. t_{ref}: reference time.

Supplementary Movies:

Supplementary_MovieS1.mov: VT corresponding to Figure 4 (VT #16).

Supplementary_MovieS2.mov: VT corresponding to Figure 5 (VT #10).

Supplementary_MovieS3.mov: VT corresponding to Figure 6 (VT #17).

References:

1. Pashakhanloo F, Herzka DA, Mori S, Zviman M, Halperin H, Gai N, Bluemke DA, Trayanova NA, Mcveigh ER. Submillimeter diffusion tensor imaging and late gadolinium enhancement cardiovascular magnetic resonance of chronic myocardial infarction. *J Cardiovasc Magn Reson*. 2017:1-14.
2. Heusch G, Skyschally A, Schulz R. The in-situ pig heart with regional ischemia / reperfusion — Ready for translation. *J Mol Cell Cardiol*. 2011;50:951-963.
3. Zhu KQ, J. G, Carrougher R, Gibran NS, Isik FF, Engrav LH. Review of the female Duroc/Yorkshire pig model of human fibroproliferative scarring. *Wound Repair Regen*. 2007;15:S32–S39.
4. Arevalo H, Plank G, Helm P, Halperin H, Trayanova N. Tachycardia in post-infarction hearts: insights from 3D image-based ventricular models. *PLoS One*. 2013;8:e68872.